EurJIC
European Journal of Inorganic Chemistry

Research Article
doi.org/10.1002/ejic.202300596

Chemistry Europe
European Chemical Societies Publishing

www.eurjic.org

Special Collection

Redox-chemistry of Pyramidanes: A DFT Study

Peter Coburger*[a]

Based on previous experimental findings, a DFT study on the redox-induced rearrangement of a series of germa-, phospha- and borapyramidanes is presented. Upon stepwise two-electron reduction, these 5-vertex *nido*-clusters are predicted to form their respective monocyclic derivatives (germole diides, (tri)phospholides and borole diides) which are formally related to the cyclopentadienide anion. Hence, it is likely that these rearrangements are a common reactivity of pyramidanes. Based on the calculations, the oxidation of these monocyclic derivatives is expected to result in the formation of meta-stable dimers for germanium and phosphorus species, and monomeric borole derivatives for boron species. Consequently, investigating the redox chemistry of pyramidanes presents an exciting opportunity to discover new and unique main-group species.

Introduction

Pyramidane, [C(η^4-C_4H_4)], is a 5-vertex *nido*-cluster where all four substituents of the apical C atom lie within the same hemisphere. For such a structure, the term "inverted tetrahedral" environment was coined by Wiberg.[1] Due to the unusual bonding situation, pyramidane has attracted attention from theoretical chemists starting from the 1970s.[2–7] While the parent species [C(η^4-C_4H_4)] remains elusive as of today, several heteroatom-substituted derivatives were prepared in the last two decades. These derivatives might also be regarded as complexes where a dianionic, four membered base acts as a 6π-donor toward BCl^{2+},[8] E^{2+} (E = Si, Ge, Sn, Pb)[9–13] or P^{3+}.[14,15] As such, most of these derivatives feature either a $[tBu_2C_2P_2]^{2-}$ or $[TMS_4C_4]^{2-}$ base. Recently, the germapyramidane **$[Ge(\eta^4\text{-}IPr_2C_2P_2)]^{2+}$** was reported, which features the neutral $IPr_2C_2P_2$ base (IPr = 1,3-bis(2,6-diisopropylphenyl)imidazolium-2-ylidene).[16] This base is formally derived from replacing the *tert*-butyl groups in $[tBu_2C_2P_2]^{2-}$ with imidazolium moieties (Scheme 1). Note, that a second borapyramidane derivative with an unusual boryl-substituted C_4 base, **$[BC_6F_5(\eta^4\text{-}TMS_2R'R''C_4)]$** (R′ = H, R″ = $B(C_6F_5)_2$) was reported as well.[17]

In comparison to their structural diversity, little is known about the redox properties of pyramidanes. The first example was reported in 2018 by Lee and coworkers:[8] Reduction of the borapyramidane **$[BCl(\eta^4\text{-}C_4TMS_4)]$** (Scheme 1) with elemental lithium led to a facile rearrangement of the cluster to the planar, aromatic borole diide $[C_4TMS_4BCl]^{2-}$. In 2022, a similar behavior was reported for the dicationic germapyramidane **$[Ge(\eta^4\text{-}IPr_2C_2P_2)]^{2+}$** (Scheme 1): Two-electron reduction of

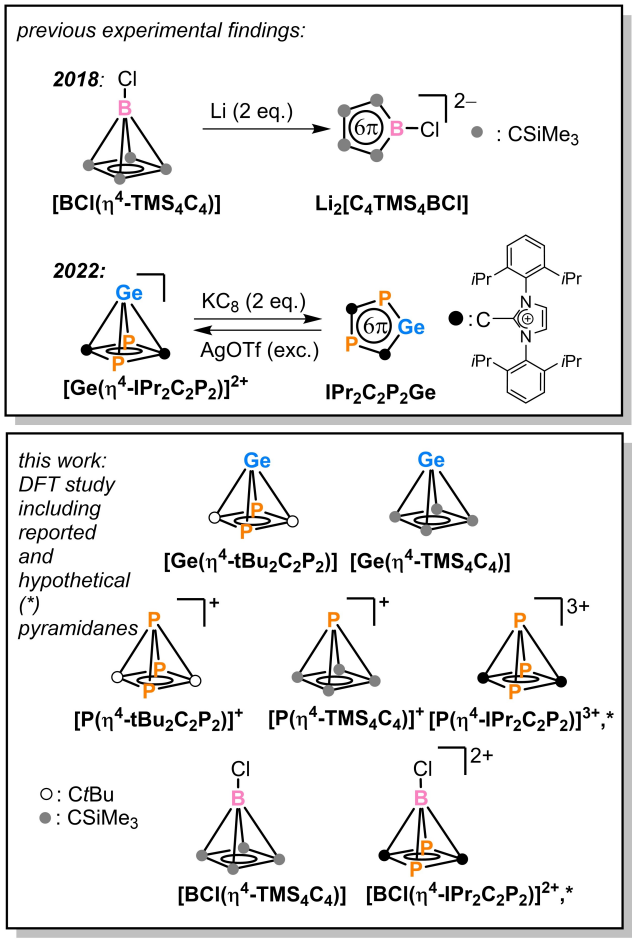

Scheme 1. Redox chemistry of **$[BCl(\eta^4\text{-}C_4TMS_4)]$** and **$[Ge(\eta^4\text{-}IPr_2C_2P_2)]^{2+}$** (top, counterions ($[C_4TMS_4BCl]^{2-}$: Li^+, **$[Ge(\eta^4\text{-}IPr_2C_2P_2)]^{2+}$**: $BArF_{24}^-$ or OTf^-) are omitted for clarity). Bottom: pyramidane derivatives investigated in this computational study.

[a] *Dr. P. Coburger*
Faculty of Chemistry, TU Munich
Lichtenbergstraße 4, 85748 Garching (Germany)
E-mail: peter.coburger@tum.de
Homepage: http://www.professoren.tum.de/en/tum-junior-fellows/coburger-peter

Supporting information for this article is available on the WWW under https://doi.org/10.1002/ejic.202300596

Part of the Special Collection on "Inorganic Reaction Mechanisms".

$[Ge(\eta^4\text{-}IPr_2C_2P_2)]^{2+}$ afforded the planar aromatic bis(imidazolium)-substituted germole diide $IPr_2C_2P_2Ge$. This process is reversible, i.e., oxidation of $IPr_2C_2P_2Ge$ results in formation of $[Ge(IPr_2C_2P_2)]^{2+}$ and the mechanism was deduced using experimental and computational methods.[16] Both $[C_4TMS_4BCl]^{2-}$ and $IPr_2C_2P_2Ge$ may formally be regarded as main-group analogues of the ubiquitous cyclopentadienide anion. In addition, it is interesting to note that the related cyclopentadienide derivative of $[P(\eta^4\text{-}tBu_2C_2P_2)]^+$ is also known.[14] However, it was not prepared via a two-electron reduction of the parent pyramidane.

The redox-induced transformations of five-vertex clusters into aromatic five-membered planar ring systems is of fundamental interest as pointed out by Canac and Bertrand.[18] Such a reaction links two concepts which relate the valence electron count of a compound to their structure/properties, namely the Wade-Mingos-Rudolph rules (clusters) and the Hückel-rules (aromaticity of cyclic species).

In light of these findings, two questions arise. First, if the reduction of pyramidane derivatives would generally induce the rearrangement to the respective cyclopentadienide analogue and secondly, if the oxidation of those species would regenerate the parent pyramidane. To provide a possible answer, a detailed DFT study is presented here. The study in total covers seven pyramidanes with three different apexes (Ge^{2+}, P^{3+} and BCl^{2+}) based on the common $[tBu_2C_2P_2]^{2-}$ and $[TMS_4C_4]^{2-}$ bases as well as the neutral $IPr_2C_2P_2$ base (Scheme 1); the five known pyramidanes $[Ge(\eta^4\text{-}tBu_2C_2P_2)]$, $[Ge(\eta^4\text{-}TMS_4C_4)]$, $[P(\eta^4\text{-}tBu_2C_2P_2)]^+$, $[P(\eta^4\text{-}TMS_4C_4)]^+$ and $[BCl(\eta^4\text{-}TMS_4C_4)]$, as well as the hypothetical species $[P(\eta^4\text{-}IPr_2C_2P_2)]^{3+}$ and $[BCl(\eta^4\text{-}IPr_2C_2P_2)]^{2+}$.

Results and Discussion

Throughout the computational study, the ORCA[19] program package was used and structures and thermal corrections were obtained using B97-3c.[20] Dipp substituents in species based on the $IPr_2C_2P_2$ base were replaced by Ph groups to save computational cost. For the calculation of final electronic energies, two functionals were considered. First, the *meta*-GGA functional M06 L,[21] as it was used to investigate the dicationic germapyramidane $[Ge(\eta^4\text{-}IPr_2C_2P_2)]^{2+}$ and yielded a good agreement with the experimental data, considering redox-potentials and kinetic barriers. Secondly, the double-hybrid functional PWPB95[22] was used in its DLPNO variant. The original PWPB95 functional was used to study borapyramidanes and yielded energies close to the accurate DLPNO-CCSD(T)[23,24] method in case of $[BCl(\eta^4\text{-}TMS_4C_4)]$.[17] Both functionals were used in combination with the def2-TZVPP basis,[25] the respective dispersion correction[26,27] and the CPCM solvent model for acetonitrile.[28] The DLPNO-PWPB95 results will be discussed at the end of results and discussion section.

The obtained reduction pathways for the germanium species $[Ge(\eta^4\text{-}tBu_2C_2P_2)]$ and $[Ge(\eta^4\text{-}TMS_4C_4)]$ are similar to the one found for the dicationic germapyramidane $[Ge(\eta^4\text{-}IPr_2C_2P_2)]^{2+}$ (Schemes 2 and 3).Two single-electron reduction steps convert the *nido*-clusters first into the radical anions $[Ge(\eta^3\text{-}tBu_2C_2P_2)]^{\bullet-}$ and $[Ge(\eta^2\text{-}TMS_4C_4)]^{\bullet-}$ and subsequently into the *arachno*-clusters $[Ge(\eta^3\text{-}tBu_2C_2P_2)]^{2-}$ and $[Ge(\eta^2\text{-}TMS_4C_4)]^{2-}$, respectively. As can be seen from the hapticity changes, reduction of these pyramidanes is accompanied by vertex opening of the clusters. Compared to the dicationic germapyramidane $[Ge(\eta^4\text{-}IPr_2C_2P_2)]^{2+}$, the reduction potentials are, as expected, more negative (−1.2 and −1.4 V vs. −2.8 and −3.0 V for $[Ge(\eta^4\text{-}tBu_2C_2P_2)]$, −3.3 and −3.4 V for $[Ge(\eta^4\text{-}TMS_4C_4)]$). Next, the reduced clusters undergo an exergonic rearrangement via TS_{2e} to form the aromatic germole-diides $[tBu_2C_2P_2Ge]^{2-}$ and $[TMS_4C_4Ge]^{2-}$. The activation barriers are lowered compared to $[Ge(\eta^3\text{-}IPr_2C_2P_2)]$ (31.4 vs. 30.0 for $[Ge(tBu_2C_2P_2)]^{2-}$ and 26.5 for $[Ge(TMS_4C_4)]^{2-}$, all values in kcal·mol^{-1}). Thus, a reduction-induced rearrangement of the germapyramidanes to dianionic germole diides upon two-electron reduction seems possible. Note, that according to the Eyring equation, an activation barrier of 26.5 kcal·mol^{-1} corresponds to a half-life of 26 days at 300 K. However, small changes in the activation barrier cause large changes in the calculated half-lifes. For example, the rearrangement of

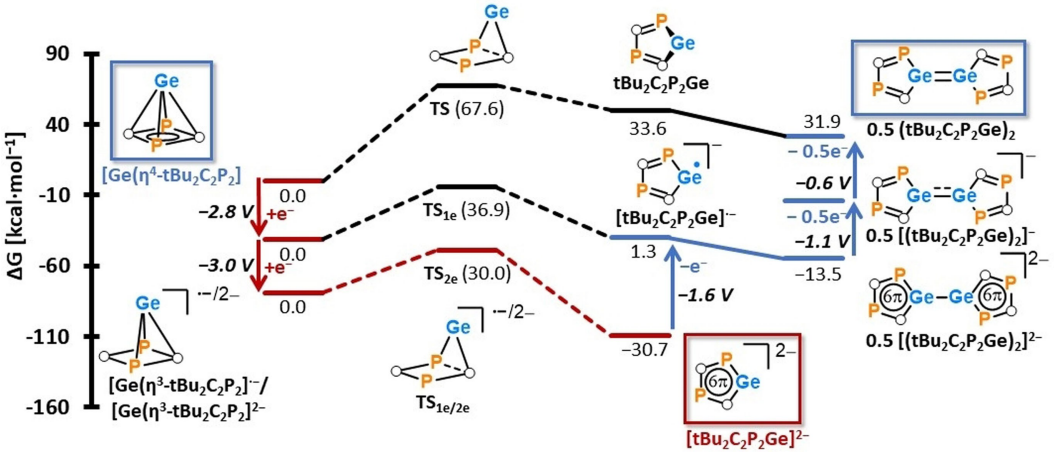

Scheme 2. Proposed redox-chemistry of $[Ge(\eta^4\text{-}tBu_2C_2P_2)]$. All calculated potentials are given in V *vs.* Fc/Fc^+.

Research Article
doi.org/10.1002/ejic.202300596

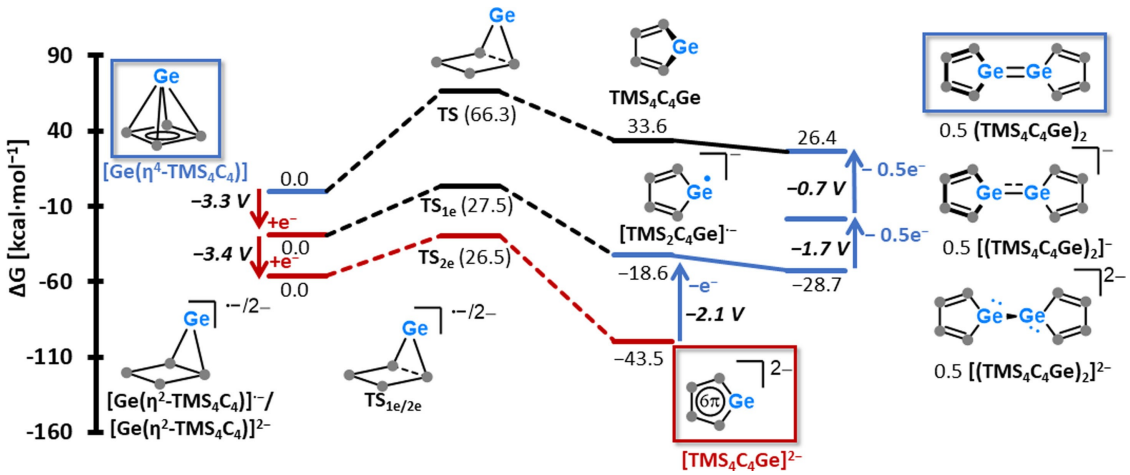

Scheme 3. Proposed redox-chemistry of **[Ge(η⁴-TMS₄C₄)]**. All calculated potentials are given in V *vs.* Fc/Fc^{+}.

[Ge(η³-IPr₂C₂P₂], for which a barrier of 31.4 kcal·mol^{-1} was calculated, is completed within 2 days.[16]

Thus, comparably small inaccuracies in the calculated activation barriers will lead to large discrepancies between calculated and measured reaction times. Therefore, throughout the study, comparisons of calculated activation barriers will be used to make a qualitative estimate about the reaction times relative to the ones calculated for the original **[Ge(η⁴-IPr₂C₂P₂)]²⁺** system.

Overall, the reduction-induced rearrangements of the germanium species follow an electron transfer/electron transfer/chemical reaction (EEC) mechanism (marked in red in Schemes 2 and 3). Note, that in principle, already the one-electron reduced germanium clusters **[Ge(η³-tBu₂C₂P₂)]•⁻** and **[Ge(η²-TMS₄C₄)]•⁻** might rearrange to five-membered ring species: At the one-electron reduced stage, the rearrangement to the planar radical species **[tBu₂C₂P₂Ge]•⁻** and **[TMS₄C₄Ge]•⁻** via **TS$_{1e}$** might occur.

These radicals carry a significant spin population on the germanium atoms (0.45 and 0.54, see the SI, section 2 for a depiction) and might thus rapidly form the dimeric digermole diides **[(tBu₂C₂P₂Ge)₂]²⁻** and **[(TMS₄C₄Ge)₂]²⁻** in an exergonic Ge–Ge bond formation reaction according to **[XGe]•⁻**→0.5 **[(XGe)₂]²⁻** ($\Delta_R G^\circ = -14.8$ kcal·mol^{-1} for X=tBu₂C₂P₂ and −10.1 kcal·mol^{-1} for X=TMS₄C₄). The synthetic viability of this pathway was demonstrated for **[Ge(η⁴-IPr₂C₂P₂)]²⁺**. However, this reaction was rather slow, meaning that in the presence of two equivalents of reducing agent a second electron transfer to **[Ge(η³-IPr₂C₂P₂)]•⁺** proceeded much faster than the rearrangement and subsequent dimerization.[16] Indeed, also for the germanium species **[Ge(η³-tBu₂C₂P₂)]•⁻** and **[Ge(η²-TMS₄C₄)]•⁻** the transition states **TS$_{1e}$** for the rearrangement to **[tBu₂C₂P₂Ge]•⁻** and **[TMS₄C₄Ge]•⁻** are significant and even higher than **TS$_{2e}$**.

While the planar radical species **[tBu₂C₂P₂Ge]•⁻** and **[TMS₄C₄Ge]•⁻** might not be of relevance for the two-electron reductive pathway of the germapyramidanes, they are indeed relevant intermediates in the oxidative pathways (marked in blue in Schemes 2 and 3). One-electron oxidation of the dianions **[tBu₂C₂P₂Ge]²⁻** and **[TMS₄C₄Ge]²⁻** at −1.6 V and −2.1 V, respectively, leads to the radical anions **[tBu₂C₂P₂Ge]•⁻** and **[TMS₄C₄Ge]•⁻** and after rapid dimerization to the dimeric digermole diides **[(tBu₂C₂P₂Ge)₂]²⁻** and **[(TMS₄C₄Ge)₂]²⁻** (vide supra). The digermole diides are then further oxidized to the neutral digermenes **(tBu₂C₂P₂Ge)₂** and **(TMS₄C₄Ge)₂** in two single-electron steps (**[(tBu₂C₂P₂Ge)₂]²⁻**: −1.1 and −0.6 V, **[(TMS₄C₄Ge)₂]²⁻**: −1.7 and −0.7 V). These digermenes might dissociate in a slightly endergonic reaction to the respective germylenes according to 0.5 **(XGe)₂**→**XGe** ($\Delta_R G^\circ = 1.7$ kcal·mol^{-1} for X=tBu₂C₂P₂ and 7.2 kcal·mol^{-1} for X=TMS₄C₄). These germylenes can then rearrange to the initial germapyramidanes via **TS**. Relative to the monomeric germylenes **XGe**, the activation barrier $\Delta G^{\ddagger}$ is 34.0 kcal·mol^{-1} for X=tBu₂C₂P₂ and 32.7 kcal·mol^{-1} for X=TMS₄C₄. The calculated total values for this respective step in the redox-cycle of the dicationic germapyramidane **[Ge(IPr₂C₂P₂)]²⁺** are $\Delta_R G^\circ =$ 7.4 kcal·mol^{-1} for the dissociation step and $\Delta G^{\ddagger} =$ 16.4 kcal·mol^{-1} for the activation barrier. Thus, the significantly higher activation barriers found for **(tBu₂C₂P₂Ge)₂** and **(TMS₄C₄Ge)₂** indicate that the digermenes, while being thermodynamically unstable with respect to the formation of the respective pyramidanes, might represent *meta*-stable species.

Moving from group 14 to group 15, the cationic phosphapyramidanes **[P(η⁴-tBu₂C₂P₂)]⁺** and **[P(η⁴-TMS₄C₄)]⁺** were investigated next. The reductive pathways are similar to those calculated for the analogues germapyramidanes (marked in red in Scheme 4 and 5): Two-single electron reduction steps open the phosphapyramidanes to the anionic clusters **[P(η²-tBu₂C₂P₂)]⁻** and **[P(η²-TMS₄C₄)]⁻**. As expected, the cationic charge of those pyramidanes increases the reduction potential compared to the neutral germapyramidanes (−1.0 and −1.7 V for **[P(η⁴-tBu₂C₂P₂)]⁺**, −1.8 and −1.8 V for **[P(η⁴-TMS₄C₄)]⁺**). Subsequently, the reduced clusters rearrange via **TS$_{2e}$** to the respective monocyclic ring species, namely the (tri)phospholides **[tBu₂C₂P₃]⁻** and **[TMS₄C₄P]⁻**. For **[P(η²-tBu₂C₂P₂)]⁻**, the activation barrier for the rearrangement

Research Article
doi.org/10.1002/ejic.202300596

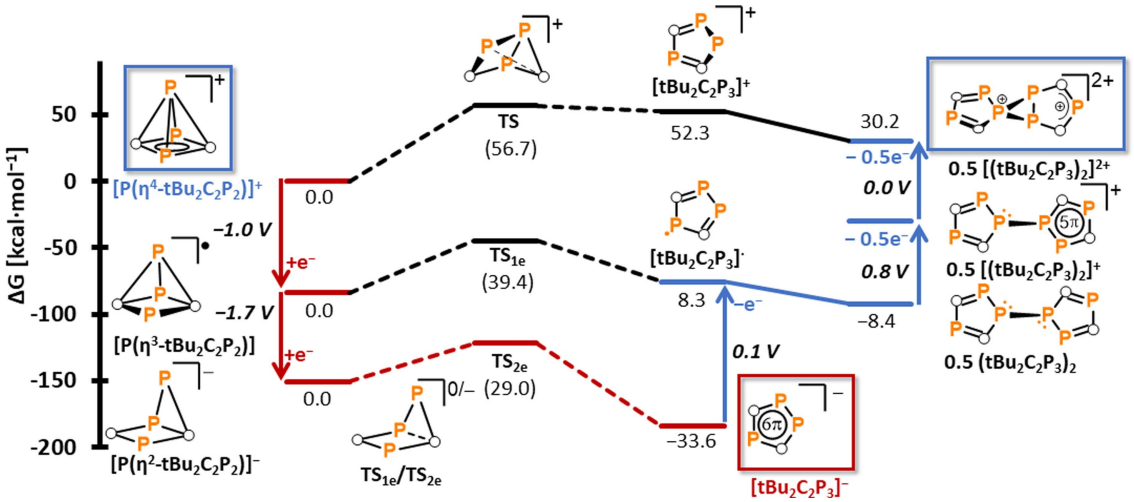

Scheme 4. Proposed redox-chemistry of $[P(\eta^4\text{-}tBu_2C_2P_2)]^+$. All calculated potentials are given in V *vs.* Fc/Fc^+.

to $[tBu_2C_2P_3]^-$ is lowered compared to $[Ge(IPr_2C_2P_2)]$ (31.4 vs. 29.0 kcal·mol^{-1}) again indicating the possibility of a facile reaction. In contrast, the respective barrier for $[P(\eta^2\text{-}TMS_4C_4)]^-$ is higher (33.5 kcal·mol^{-1}) indicating that the rearrangement to $[TMS_4C_4P]^-$ might be slower or not even feasible in this case.

Next, the oxidative pathways for $[tBu_2C_2P_3]^-$ and $[TMS_4C_4P]^-$ were investigated (blue in Schemes 4 and 5). Again, these are similar to the respective pathways calculated for the germanium species: One-electron oxidation of the (tri)phospholides results in the formation of the radical species $[tBu_2C_2P_3]^\bullet$ and $[TMS_4C_4P]^\bullet$ (see the SI section 2 for a depiction of the spin density). These form the di(triphosphole) $(tBu_2C_2P_3)_2$ and diphosphole $(TMS_4C_4P)_2$ in an exergonic reaction (−16.7 and −11.4 kcal·mol^{-1}).[29] Next, these neutral species are oxidized in two single-electron steps. Interestingly, the two resulting dications, $[(tBu_2C_2P_3)_2]^{2+}$ and $[(TMS_4C_4P)_2]^{2+}$, show completely different structures. $[(TMS_4C_4P)_2]^{2+}$ might be best described as a diphosphole dication, where one lone pair of electrons had been formally removed from the parent diphosphole. In contrast, a polycyclic structure was obtained in the geometry optimization of $[(tBu_2C_2P_3)_2]^{2+}$. Notwithstanding their structural differences, both dicationic species are predicted to form the respective monomers $[tBu_2C_2P_3]^{2+}$ and $[TMS_4C_4P]^{2+}$ in an endergonic reaction, followed by rearrangement to the original phosphapyramidanes. As for the germanium species, the rather high total activation barriers, i.e. the energetic difference between **TS** and $[(tBu_2C_2P_3)_2]^{2+}/[(TMS_4C_4P)_2]^{2+}$, respectively indicate that these dications are again *meta*-stable species.

The final considered phosphapyramidane is the hypothetical trication $[P(\eta^4\text{-}IPr_2C_2P_2]^{3+}$ (Scheme 6). The reductive pathway differs slightly from the already discussed examples. One- and two-electron reduction of $[P(\eta^4\text{-}IPr_2C_2P_2]^{3+}$ produces the opened clusters $[P(\eta^3\text{-}IPr_2C_2P_2]^{2+}$ and $[P(\eta^3\text{-}IPr_2C_2P_2]^{+}$, respectively. In contrast to the previous examples, $[P(\eta^3\text{-}IPr_2C_2P_2]^{+}$ rearranges to the bis(imidazolium)-substituted triphospholide $[IPr_2C_2P_3]^{+}$ in a two-step process. First, one C—P bond of the

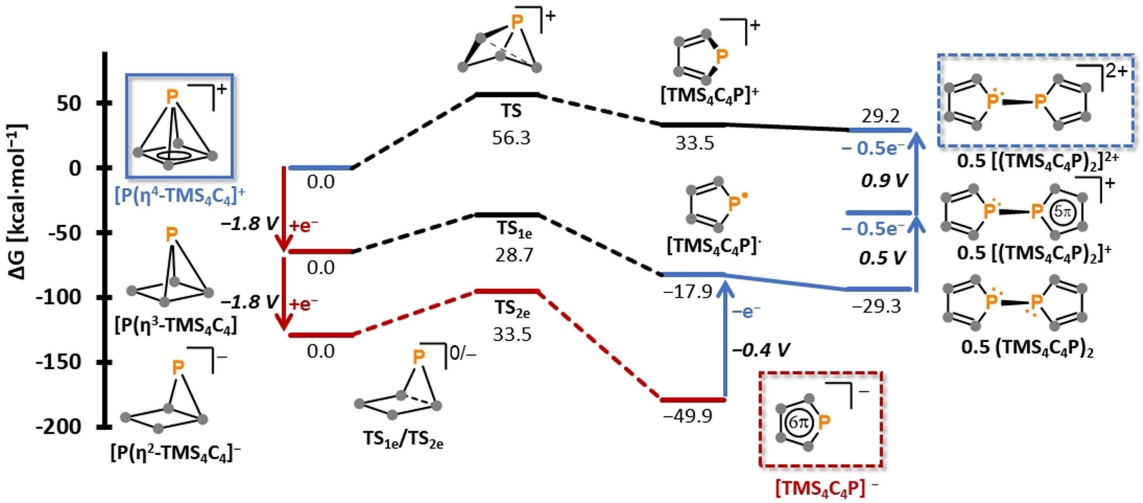

Scheme 5. Proposed redox-chemistry of $[P(\eta^4\text{-}TMS_4C_4)]^+$. All calculated potentials are given in V *vs.* Fc/Fc^+.

Research Article
doi.org/10.1002/ejic.202300596

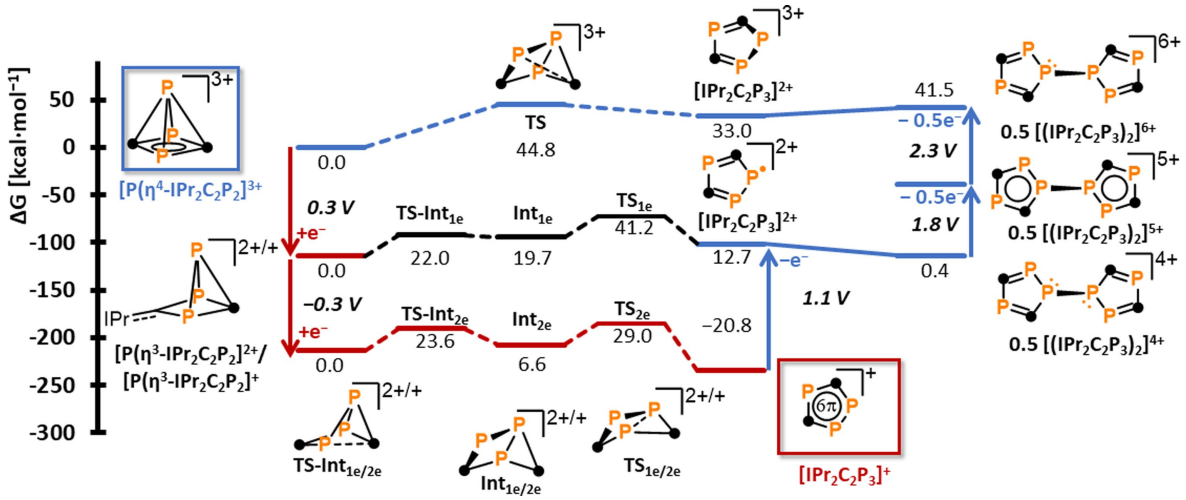

Scheme 6. Proposed redox-chemistry of $[P(\eta^4\text{-}IPr_2C_2P_2)]^{3+}$. All calculated potentials are given in V *vs.* Fc/Fc^+. The circles in the dimeric pentacation denote delocalization of the unpaired electron over the whole molecule.

$IPr_2C_2P_2$ base is broken leading to the intermediate $\mathbf{Int_{2e}}$. The five-membered heterocycle $[\mathbf{IPr_2C_2P_3}]^+$ is then formed via the transition state $\mathbf{TS_{2e}}$. This step is rate-determining and has a total activation barrier of 29.0 kcal·mol^{-1}.

This barrier is again lower than the one reported for $[\mathbf{Ge(\eta^3\text{-}IPr_2C_2P_2)}]$ indicating an efficient rearrangement process. The rearrangement of the one-electron reduced species $[\mathbf{P(\eta^3\text{-}IPr_2C_2P_2)}]^{2+}$ proceeds in a similar two-step process, but again, the very high total activation barrier of 41.2 kcal·mol^{-1} makes this process not competitive with a rapid second reduction to the two-electron reduced species $[\mathbf{P(\eta^3\text{-}IPr_2C_2P_2)}]^+$.

Until the last step, the oxidative pathway calculated for $[\mathbf{IPr_2C_2P_3}]^+$ is identical to those discussed for the other phosphapyramidanes: Oxidation of $[\mathbf{IPr_2C_2P_3}]^+$ results in formation of the radical species $[\mathbf{IPr_2C_2P_3}]^{2+}$ which dimerizes to $[(\mathbf{IPr_2C_2P_3})_2]^{4+}$. This tetracation is subsequently oxidized in two single electron steps. Due to the high positive charge, the calculated potentials for these steps are quite high (1.8 and 2.3 V, respectively). The high charge of the resulting hexacation in addition renders the dissociation into two tricationic monomers exergonic (0.5 $[(\mathbf{IPr_2C_2P_3})_2]^{4+} \rightarrow [\mathbf{IPr_2C_2P_3}]^{3+}$, $\Delta_R G^\circ = -8.5$ kcal·mol^{-1}). Rearrangement of this monomer to the phosphapyramidane $[\mathbf{P(\eta^4\text{-}IPr_2C_2P_2)}]^{3+}$ proceeds via a low barrier of only 11.8 kcal/mol indicating that the redox-cycle for this particular pyramidane can be closed, i.e. oxidation of the triphospholide $[\mathbf{IPr_2C_2P_3}]^+$, at least *in silico*, results in the rearrangement to the phosphapyramidane.

Finally, pyramidanes with an apical BCl unit were investigated. For the borapyramidane $[\mathbf{BCl(TMS_4C_4)}]$, the potentials of the calculated single-electron reduction steps are similar to the related germapyramidane $[\mathbf{Ge(TMS_4C_4)}]$ (−3.6 and −3.6 V vs. −3.3 and −3.4 V, Scheme 7). However, the kinetic barriers for the rearrangement of the thereby formed negatively charged clusters to their planar, five-membered counterparts are strongly reduced compared to the respective germanium

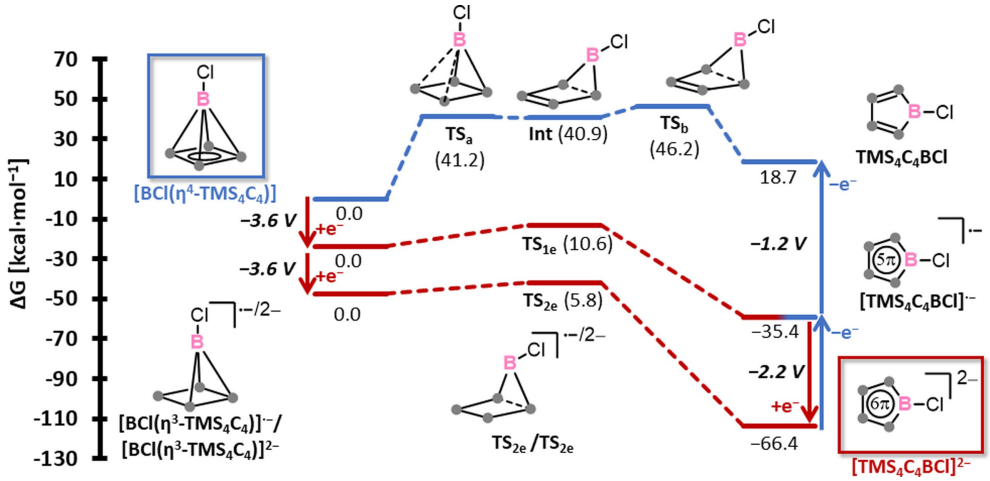

Scheme 7. Proposed redox-chemistry of $[\mathbf{BCl(TMS_4C_4)}]$. All calculated potentials are given in V *vs.* Fc/Fc^+.

Research Article
doi.org/10.1002/ejic.202300596

counterparts ($\Delta G^{\ddagger} = 10.6$ kcal·mol^{-1} for **[BCl(TMS$_4$C$_4$)]$^{\bullet-}$** and 5.8 kcal·mol^{-1} for **[BCl(TMS$_4$C$_4$)]$^{2-}$**).

Thus, the redox process **[BCl(TMS$_4$C$_4$)]** + 2e→**[TMS$_4$C$_4$BCl]$^{2-}$** might follow the EEC mechanism established for the germanium and phosphorus species. Since, unlike for the phosphorus and germanium species, **TS$_{1e}$** is very low in energy, already the one-electron reduced cluster might rearrange forming the planar borole radical anion **[TMS$_4$C$_4$BCl]$^{\bullet-}$** This radical is subsequently reduced to the aromatic borole diide **[TMS$_4$C$_4$BCl]$^{2-}$** at −2.2 V (see the red paths in Scheme 4). The latter path corresponds to an ECE mechanism.

For both the EEC and ECE mechanism, the calculated low kinetic barriers agree with the observed rapid formation of **[TMS$_4$C$_4$BCl]$^{2-}$** when **[BCl(η^4-TMS$_4$C$_4$)]** is reduced with lithium.[8] The oxidation of the borole diide **[TMS$_4$C$_4$BCl]$^{2-}$** is predicted to proceed rather differently compared to the formally related germole diides and phospholides: Single-electron oxidation of **[TMS$_4$C$_4$BCl]$^{2-}$** leads to the planar radical anion **[TMS$_4$C$_4$BCl]$^{\bullet-}$** which is now stable towards dimerization (see the SI section 5). In part, this might be explained by the rather delocalized spin-density in **[TMS$_4$C$_4$BCl]$^{\bullet-}$**, compared to the respective planar germole radical anions (see the SI, section 2). Further oxidation of **[TMS$_4$C$_4$BCl]$^{\bullet-}$** at −1.2 V then leads to the neutral borole **TMS$_4$C$_4$BCl** which again is stable toward dimerization. The rearrangement of the borole **TMS$_4$C$_4$BCl** to the borapyramidane **[BCl(η^4-TMS$_4$C$_4$)]** is predicted to proceed in two steps: The endothermic isomerization to the housane intermediate **Int** (via **TS$_b$**) which subsequently forms the borapyramidane via **TS$_a$**.[30] A similar two-step mechanism was calculated for the borapyramidane **[BC$_6$F$_5$(η^4-TMS$_2$R′R″C$_4$)]** reported by Erker and coworkers.[17] The rate-limiting step in this sequence is the formation of the housane **Int** which, relative to the borole **TMS$_4$C$_4$BCl**, has a total activation barrier of $\Delta G^{\ddagger} =$ 27.5 kcal·mol^{-1}. Thus, like the digermenes discussed earlier (vide supra), the borole **TMS$_4$C$_4$BCl** corresponds to a *meta*-stable species which might be observable experimentally.

For the reduction of the hypothetical dicationic borapyramidane **[BCl(η^4-IPr$_2$C$_2$P$_2$)]$^{2+}$**, again two reductive mechanisms, EEC and ECE are plausible based on the calculated activation barriers (see the red paths in Scheme 8). Similar to the borole diide **[TMS$_4$C$_4$BCl]$^{2-}$**, the neutral bis(imidazolium)-substituted borole diide **IPr$_2$C$_2$P$_2$BCl** is predicted to be oxidized in two single-electron steps at −0.5 and 0.4 V with no dimeric species being involved (see the SI section 5). However, the final rearrangement of the dicationic borole **[IPr$_2$C$_2$P$_2$BCl]$^{2+}$** to the borapyramidane **[BCl(η^4-IPr$_2$C$_2$P$_2$)]$^{2+}$** is found to proceed in a single step, namely via the triplet transition state **TS**. The activation barrier for this process is rather high ($\Delta G^{\ddagger} = 29.3$ kcal·mol^{-1}). Therefore, similar to the neutral borole **TMS$_4$C$_4$BCl**, the dicationic borole **[IPr$_2$C$_2$P$_2$BCl]$^{2+}$** is a *meta*-stable species. Notably, **TS** and thus the activation barrier is raised by +12.5 kcal·mol^{-1} using DLPNO-PWPB95 (see below and the SI, section 3), and therefore this method predicts **[IPr$_2$C$_2$P$_2$BCl]$^{2+}$** to be even more kinetically stable towards rearrangement to the respective pyramidane. Thus, **[IPr$_2$C$_2$P$_2$BCl]$^{2+}$** might be an experimentally accessible, *meta*-stable borole. The predicted *meta*-stability of the boroles is corroborated by experimental findings by Erker and coworkers: The pyramidane **[BC$_6$F$_5$(η^4-TMS$_2$R′R″C$_4$)]**, while stable at ambient temperatures, could indeed be interconverted to the borole **TMS$_2$R′R″C$_4$BC$_6$F$_5$** upon heating. This borole was characterized as its SMe$_2$ adduct, which in turn could be converted to the pyramidane **[BC$_6$F$_5$(η^4-TMS$_2$R′R″C$_4$)]** by radiation with UV light.[17]

In this computational study, DLPNO-PWPB95 was used as a second functional (see the SI, section 3). Compared to M06 L, all redox potentials are, on average, lowered by 0.5 V. The activation barriers **TS$_{1e}$** and **TS$_{2e}$** are reproduced with a mean average deviation (MAD) of 4.8 kcal·mol^{-1} for **TS$_{1e}$** and a MAD of 2.4 kcal·mol^{-1} for **TS$_{2e}$**. Thus, especially the values of **TS$_{2e}$** are in qualitative agreement with the M06 L data, supporting the facile rearrangement of two-electron reduced clusters to their cyclopentadienide analogues. In contrast, the transition states

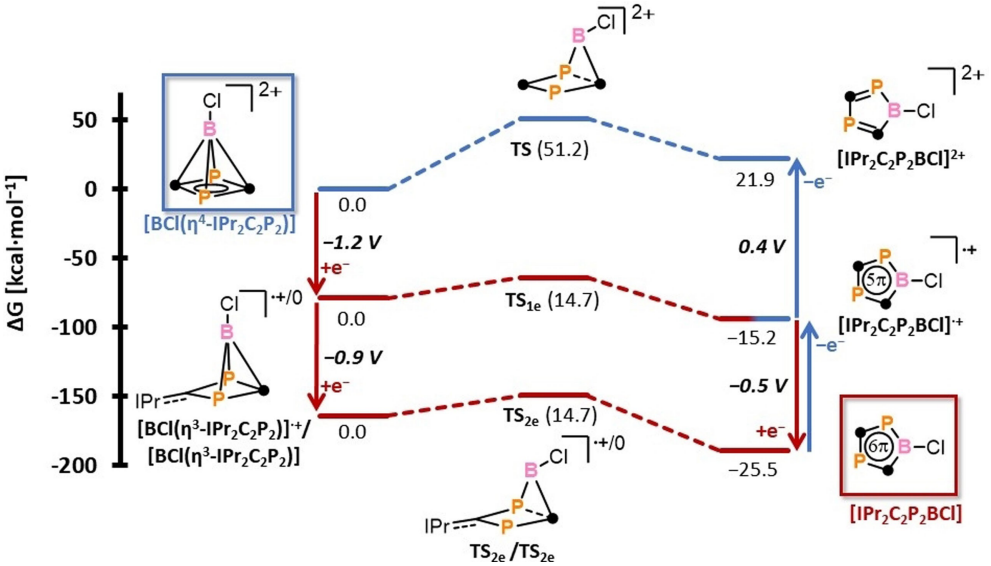

Scheme 8. Proposed redox-chemistry of **[BCl(IPr$_2$C$_2$P$_2$)]$^{2+}$**. All calculated potentials are given in V *vs.* Fc/Fc$^+$.

Research Article
doi.org/10.1002/ejic.202300596

TS are estimated to be higher by 5.9 kcal·mol^{-1} on average. Thus, the oxidized species are predicted to be even more kinetically stable towards rearrangement to the respective pyramidanes.

Conclusions

In summary, the redox chemistry of seven pyramidane derivatives was investigated computationally with the focus on two particular questions: First, if the reduction of pyramidane derivatives would generally induce the rearrangement to monocyclic species and secondly, if the oxidation of those species would regenerate the parent pyramidane.

In all the clusters that were examined, it was found that the two-electron reduction of pyramidanes could potentially lead to the formation of *arachno*-clusters as predicted by the Wade-Mingos rules. However, thermodynamically, the isomerization to the respective monocyclic, aromatic species was calculated to be more favorable. With one exception ($[\mathbf{P(\eta^2\text{-}TMS_4C_4)}]^-$) these isomerizations are predicted to occur faster than the experimentally observed reaction $[\mathbf{Ge(\eta^4\text{-}IPr_2C_2P_2)}]^{2+}$ $2e^- \rightarrow$ $\mathbf{IPr_2C_2P_2Ge}$. To summarize the findings related to the first question, it appears that the reduction-induced rearrangement to monocyclic derivatives seems to be a common reactivity of pyramidanes.

Regarding the second question, only $[\mathbf{P(\eta^4\text{-}IPr_2C_2P_2)}]^{3+}$ was found to exhibit a fully closed redox-cycle, i.e. oxidation of the five-membered two-electron reduced derivative is indeed predicted to regenerate the pyramidane. However, it is important to highlight that the dimers found along the oxidative pathway of $[\mathbf{P(\eta^4\text{-}IPr_2C_2P_2)}]^{3+}$ are highly charged and therefore elusive and potentially unstable. Consequently, it may not be experimentally feasible to close the redox-cycle for these species. For all the other examples, the barriers for the rearrangement of two-electron oxidized cyclic species to their respective pyramidanes were found to be rather high although the pyramidanes are thermodynamically favored in all cases. Therefore, these oxidized species, which display a wide structural variety ranging from digermenes over diphosphole dications to boroles, might at least be *meta*-stable species. Therefore, the second question which was addressed in this DFT study cannot be answered conclusively based on the available data.

Thus, the synthetic exploration of the redox chemistry of pyramidanes, i.e. two-electron reduction to their planar cyclopentadienide analogues followed by two-electron oxidation seems to be a worthwhile scientific endeavor. Such experimental studies might offer synthetic access to unique main-group species with interesting properties and reactivities. Although some of those species, like the dicationic borole $[\mathbf{IPr_2C_2P_2BCl}]^{2+}$ and the highly charged dimers $[(\mathbf{IPr_2C_2P_3})_2]^{4+/5+/6+}$ are rather hypothetical, they might still be detectable in trapping experiments. It is therefore hoped that this computational study sparks further interest and progress in the field of pyramidane chemistry.

Computational Details

All calculations were carried out with the ORCA program package.[19] Density fitting techniques, also called resolution-of-identity approximation (RI),[31] were used for all B97-3c and M06 L calculations, whereas an additional chain-of-spheres approximation for the HF exchange (RIJCOSX)[32] was used for DLPNO-PWPB95 calculations. Atom-pairwise dispersion corrections were used for all DFT calculations [B97-3c, DLPNO-PWPB95: D3BJ, M06L: D3(0)]. All geometries and thermal corrections were obtained with the B97-3c compound method on isolated molecules using a medium-tight grid (Grid5) and TIGHTSCF convergence criteria for SCF procedure and the default convergence criteria for geometry optimisations (see an exemplary input file in the SI, section 1). Electronic energies of the optimised species were obtained using the methods described in the main text, i.e. M06L or DLPNO-PWPB95 with the appropriate dispersion correction, def2-TZVPP basis sets, TIGHTSCF convergence criteria, medium-tight grids (Grid5) and the CPCM solvent correction for acetonitrile (see the SI, section 1 for an exemplary input file). The final Gibbs free energies were subsequently obtained by adding the thermal corrections obtained with B97-3c to the electronic energies. Approximate transition state structures were obtained using the nudged elastic band method. These approximate structures were used in a subsequent saddle-point geometry optimization.

Acknowledgements

P. C. gratefully acknowledges funding from the VCI (Liebig-fellowship). Open Access funding enabled and organized by Projekt DEAL.

Conflict of Interests

The authors declare no conflict of interest.

Data Availability Statement

The data that support the findings of this study are available in the supplementary material of this article.

Keywords: Boron · cluster compounds · germanium · phosphorus · reaction mechanisms

[1] K. B. Wiberg, *Acc. Chem. Res.* **1984**, *17*, 379–386.
[2] V. I. Minkin, *Zh. Org. Khim.* **1978**, *14*, 3–15.
[3] V. I. Minkin, R. M. Minyaev, G. V. Orlova, *J. Mol. Struct.* **1984**, *110*, 241–253.
[4] E. Lewars, *J. Mol. Struct.* **1998**, *423*, 173–188.
[5] E. Lewars, *J. Mol. Struct.* **2000**, *507*, 165–184.
[6] J. P. Kenny, K. M. Krueger, J. C. Rienstra-Kiracofe, H. F. Schaefer, *J. Phys. Chem. A* **2001**, *105*, 7745–7750.
[7] R. R. Aysin, S. S. Bukalov, *Mendeleev Commun.* **2021**, *31*, 481–483.
[8] V. Ya. Lee, H. Sugasawa, O. A. Gapurenko, R. M. Minyaev, V. I. Minkin, H. Gornitzka, A. Sekiguchi, *J. Am. Chem. Soc.* **2018**, *140*, 6053–6056.
[9] M. D. Francis, P. B. Hitchcock, *Organometallics* **2003**, *22*, 2891–2896.
[10] L. A. Leites, R. R. Aysin, S. S. Bukalov, V. Ya. Lee, H. Sugasawa, A. Sekiguchi, *J. Mol. Struct.* **2017**, *1130*, 775–780.
[11] V. Ya. Lee, Y. Ito, A. Sekiguchi, H. Gornitzka, O. A. Gapurenko, V. I. Minkin, R. M. Minyaev, *J. Am. Chem. Soc.* **2013**, *135*, 8794–8797.

[12] V. Ya. Lee, O. A. Gapurenko, Y. Ito, T. Meguro, H. Sugasawa, A. Sekiguchi, R. M. Minyaev, V. I. Minkin, R. H. Herber, H. Gornitzka, *Organometallics* **2016**, *35*, 346–356.
[13] T. Imagawa, L. Giarrana, D. M. Andrada, B. Morgenstern, M. Nakamoto, D. Scheschkewitz, *J. Am. Chem. Soc.* **2023**, *145*, 4757–4764.
[14] J. M. Lynam, M. C. Copsey, M. Green, J. C. Jeffery, J. E. McGrady, C. A. Russell, J. M. Slattery, A. C. Swain, *Angew. Chem. Int. Ed.* **2003**, *42*, 2778–2782.
[15] V. Y. Lee, H. Sugasawa, O. A. Gapurenko, R. M. Minyaev, V. I. Minkin, H. Gornitzka, A. Sekiguchi, *Chem. Eur. J.* **2016**, *22*, 17585–17589.
[16] P. Coburger, F. Masero, J. Bösken, V. Mougel, H. Grützmacher, *Angew. Chem. Int. Ed.* **2022**, *61*, e202211749.
[17] Q. Sun, C. G. Daniliuc, X. Yu, C. Mück-Lichtenfeld, G. Kehr, G. Erker, *J. Am. Chem. Soc.* **2022**, *144*, 7815–7821.
[18] Y. Canac, G. Bertrand, *Angew. Chem. Int. Ed.* **2003**, *42*, 3578–3580.
[19] F. Neese, F. Wennmohs, U. Becker, C. Riplinger, *J. Chem. Phys.* **2020**, *152*, 224108.
[20] J. G. Brandenburg, C. Bannwarth, A. Hansen, S. Grimme, *J. Chem. Phys.* **2018**, *148*, 064104.
[21] Y. Wang, X. Jin, H. S. Yu, D. G. Truhlar, X. He, *Proc. Nat. Acad. Sci.* **2017**, *114*, 8487–8492.
[22] L. Goerigk, S. Grimme, *J. Chem. Theory Comput.* **2011**, *7*, 291–309.
[23] C. Riplinger, B. Sandhoefer, A. Hansen, F. Neese, *J. Chem. Phys.* **2013**, *139*, 134101.
[24] C. Riplinger, F. Neese, *J. Chem. Phys.* **2013**, *138*, 034106.
[25] F. Weigend, R. Ahlrichs, *Phys. Chem. Chem. Phys.* **2005**, *7*, 3297–3305.
[26] S. Grimme, J. Antony, S. Ehrlich, H. Krieg, *J. Chem. Phys.* **2010**, *132*, 154104.
[27] S. Grimme, S. Ehrlich, L. Goerigk, *J. Comput. Chem.* **2011**, *32*, 1456–1465.
[28] M. Cossi, N. Rega, G. Scalmani, V. Barone, *J. Comput. Chem.* **2003**, *24*, 669–681.
[29] Note, that from inspection of the spin-density in $[tBu_2C_2P_3]^{\bullet}$, dimerization is expected to occur via the dicarbon-substituted phosphorus atoms. However, such a structure was found to be higher in gibbs free energy by 6.4 $kcal \cdot mol^{-1}$ (see the SI, section 5).
[30] Note, that the potential energy surface between $\mathbf{TS_a}$ and **Int** is very shallow and thus no real transition state could be optimised. Instead, the highest image of the minium-energy reaction path (MERP) obtained from a NEB calculation was taken as an approximation for **TSa** (see the SI section 5).
[31] R. A. Kendall, H. A. Früchtl, *Theor. Chem. Acc.* **1997**, *97*, 158–163.
[32] F. Neese, F. Wennmohs, A. Hansen, U. Becker, *Chem. Phys.* **2009**, *356*, 98–109.

Manuscript received: October 2, 2023
Revised manuscript received: November 7, 2023
Accepted manuscript online: November 10, 2023
Version of record online: December 11, 2023